Original Article

Comparison of Arc and Pulse Welding on Properties of Inconel 617

MohammadHasan Ahmadzadeh[1*], Majid Ghoreishi[1]

[1]Department of Production and Manufacturing, Khajeh Nasir Toosi University of Technology, Tehran, Iran.

Correspondence: MohammadHasan Ahmadzadeh, Department of Production and Manufacturing, Khajeh Nasir Toosi University of Technology, Tehran, Iran. mohamadhasanahmadzade14@gmail.com

ABSTRACT

The nickel-based alloy Inconel 617 has high strength and resistance to oxidation across a wide temperature range, making it suitable for combustion chambers, aerospace tubing and liners, land-based gas turbines, and biomedical applications. It is also used in power plant components in fossil and nuclear power plants. Comparison between Argon Gas Tungsten Arc Welding and Pulsed Laser Beam Welding on Mechanical Properties of Homogeneous Inconel 617 Joints. In this study, two welding methods - argon gas tungsten arc welding (GTAW) and pulsed laser beam welding - were performed on 1.5 mm thick Inconel 617 sheets welded in a butt joint configuration. Austenitic stainless steel 316 was also used as a filler material. The results showed superior performance of double-sided GTAW welding of the parts since double-sided welding helps reduce residual stresses from the base metal rolling and refinement of base metal grains in the welded area, improving mechanical properties and ultimate strength. In tensile testing, most samples failed at the joint location, as the residual stresses in the weld region were often compressive. Additionally, laser welding improved the mechanical properties of welded parts better than argon GTAW. It appears that the high heat input (and slow cooling rate) in argon GTAW potentially causes micro-segregation that leads to the deterioration of mechanical properties for the GTAW joint.

Keywords: Inconel 617, Argon gas tungsten arc welding (GTAW), Pulsed laser beam welding, Austenitic stainless steel 316.

Introduction

The construction of facilities such as steam power plants, aero, and land-based gas turbines, aircraft, etc., is considered one of the most important basic infrastructures in any country. What is important in the construction of these critical facilities is attention to increasing two factors: pressure and temperature [1]. Transfer liners in these facilities require high temperatures, high corrosion resistance levels, and high fatigue strength and stress rupture resistance [2]. In such cases, nickel-based superalloys with high strength and surface stability at high pressures and temperatures are very suitable [2, 3].

Inconel 617 is a nickel-based solid solution superalloy with a face-centered cubic (FCC) crystal structure. This high-temperature alloy is widely used in applications where operating temperatures exceed 700°C, including aircraft and land-based gas turbines [4, 5]. The key properties that make Inconel 617 well-suited for these high-temperature environments are its corrosion resistance, mechanical strength, thermal stability, and creep resistance at elevated temperatures [6, 7]. The superior high-temperature mechanical properties of Inconel 617 are attributed to precipitation strengthening from carbides and intermetallic phases such as M23C6, M6C, and MX [8].

Specific applications of Inconel 617 include combustion chambers, transition ducts, and exhaust components in gas turbine engines where temperatures can reach or exceed 700 °C [9]. This nickel alloy also exhibits excellent hot corrosion resistance in many oxidizing and reducing environments due to its composition's synergistic effects of chromium, aluminum, and molybdenum [10]. Across a wide temperature range from 77-1093 K, Inconel 617 retains its tensile properties with minimal variation even after long-term exposure to environments such as salt-vacuum [11]. However, welding and repair of Inconel 617 remains challenging because of its susceptibility to weld cracking and heat-affected zone damage during fabrication, post-weld heat treatment, and subsequent handling [12].

Various welding processes can significantly influence the microstructural and mechanical properties of Inconel 617 nickel-based superalloy. Kumar and Balasubramanian [1] conducted experiments on the high-temperature tensile behavior of multi-pass pulsed cold metal transfer welded Inconel 617 alloy. They observed that weld bead width, penetration depth, weld deposit geometry, and heat-affected zone (HAZ) dimensions exhibited a direct correlation to wire feed rate based on their results. Bending tests of the welded joints also indicated good ductility without cracking after pulsed cold metal transfer welding. In another study, Mandal et al. [13] extensively characterized the evolution of microstructural and mechanical properties of tungsten inert gas (TIG) welded Inconel 617 superalloy. Their findings revealed that the impact toughness of Inconel 617 was significantly reduced after post-weld heat treatment for different soaking times. This degradation was attributed to coarsening of carbides at grain boundaries and embrittlement effects during TIG welding. Sun et al. [6] conducted detailed investigations on the weldability, resultant microstructure, and mechanical properties, including tensile strength of thick Inconel 617 alloy plates joined using a narrow gap laser welding process. Their results showed that the geometry of U-shaped or V-shaped filler wire strongly influenced mitigating weld defects. Although the tensile strength was found to decrease with increasing temperature, the fusion zone exhibited higher strength relative to the base metal due to the presence of fine dimples based on microscopy. In the study by Esmaili et al. [14] a transient liquid phase bonding vacuum brazing process was utilized to join Inconel 617 superalloy using Ni-Cr-Si-Fe-B filler metal successfully. They reported that the maximum shear strength of the brazed joints was obtained with optimized interlayer thickness, brazing temperature, and holding time. A comparison of gas tungsten arc welded Inconel 617 was performed by Yin et al. [15], revealing lower ultimate tensile strength but higher yield strength of the weld metal versus the base metal. However, in their investigation, the elongation of the weld metal was significantly inferior to the base metal. Finally, Mageshkumar et al. [16] analyzed the microstructure and mechanical properties of pulsed gas tungsten arc welded Inconel 617 joints. A faster cooling rate during pulsed welding resulted in a cleaner fusion zone microstructure and a narrower HAZ width. Bending tests confirmed the absence of cracks or defects in the welds produced under optimized pulsed current parameters.

Farahani et al. [17] performed a comparative study on direct current and pulsed gas tungsten arc welding of Inconel 617. The results showed that higher joint toughness and impact energy were obtained when using the pulsed gas tungsten arc welding method due to the formation of refined grains.

Despite the efforts made by researchers, understanding the role of microstructural evolution and associated mechanical properties, especially for high-temperature alloys, has always been challenging. Different welding methods have been utilized to achieve superior mechanical properties of welded joints for use in adverse temperature conditions. For joining Inconel 617 sheets, various welding methods have been used so far, such as plasma arc welding [11], gas tungsten arc welding (GTAW) [13, 18], laser welding [19, 20], activated flux tungsten inert gas welding (A-TIG) [21], electron beam welding [7], fiber laser welding [22], and more. Among these, GTAW welding offers advantages like lower heat input and higher metallurgical and visual quality when welding Inconel 617 [23]. However, the low penetration depth in this method means its use is of limited economic justification for thicker sections, as the low penetration necessitates edge preparation and filler metal, multi-pass welding, and thus a lower production rate for thick sections [18]. Regarding GTAW welding of Inconel 617, Thekkuden et al. [24] performed narrow gap TIG welding with U-groove on Inconel 617 sheets. Various welding conditions like electrode shape, welding position, arc length, heat input, and shielding gas were optimized based on a welding monitoring system. 0.96 yield strength ratio and 0.89 tensile strength ratio at room temperature were obtained under optimum welding conditions. Jeshvaghani et al. [25] investigated the microstructural and wear behavior of Inconel 617. The results showed that the microstructure of the alloy layer consisted of M23C6 carbides embedded in nickel-rich solid solution dendrites. The partially melted zone (PMZ) had a eutectic ledeburite plus martensite structure, while the heat-affected zone (HAZ) only had a martensitic structure. Also, the alloy layer's hardness and wear resistance were significantly higher than the substrate surface.

Laser welding, also known as laser beam welding (LBW), utilizes a focused beam of amplified light emitted from a laser source to fuse materials, such as metals and thermoplastics [19]. Recently, Aqeel et al. [26] conducted a comparative study on welding 10 mm thick Inconel 617 superalloy using diode laser welding, CO2-MIG hybrid laser welding, and multipass TIG welding. Their results revealed that the single-pass diode and hybrid laser welds exhibited marginally higher joint efficiency than the multipass TIG welds. Notably, the single-pass diode laser welds displayed the maximum increase in length. A major mutual advantage of the single-pass diode laser and hybrid laser methods was a significant reduction in distortion coupled with improved weld compatibility.

The summarized research highlights the indispensable role of Inconel 617 superalloys across high-temperature industrial applications. However, achieving high-quality welds in this nickel-chromium alloy while accounting for mechanical, chemical, and other performance factors poses considerable difficulties. Limited research has been done on comparing TIG and laser welding on Inconel 617. This study aims to investigate the mechanical properties of Inconel 617 superalloy in two welding methods: TIG welding with argon gas and laser welding.

Materials and Methods

This study used Inconel 617 superalloy with dimensions of 15 mm × 140 mm × 20 mm. The initial Inconel 617 samples were used in sheet form. The base metals were cleaned surface machined using a guillotine machine into 40×80 mm dimensions. Additionally, 316 stainless steel filler wire with a diameter of 2.1 mm was used to fill the created gaps. 316 stainless steel contains high levels of chromium and nickel. It also contains silicon, manganese, and carbon, with iron as the main component. The chemical compositions of Inconel 617 and the filler are shown in **Table 1**.

Table 1. Chemical composition of Inconel 617 alloy and 316 stainless steel as filler

Element	Alloy	Br	Cu	Ti	S	Si	Mg	P	Mn	Fe	C	Al	Mo	Co	Cr	Ni
percentage	Inconel 617	0.006	0.5	0.6	0.015	1	1	-	-	3	0.05-0.15	0.8-1.5	8-10	10-15	20	44.6
percentage	Stainless steel 316	-	-	-	0.030	1	-	0.045	2	26	0.08	-	2-3	-	16-18	10-14

Waterjet cutting was used to cut the sheets. The butt joint design preparation was done. A TECNO JOSH device was used for the TIG welding process with argon gas. TIG welding with argon gas was performed on one side and both sides. It should be noted that before the welding processes, to remove any surface contaminants and oxide layer on the raw samples, the joints of the samples were cleaned with a wire brush and degreased using acetone, then dried so that the samples were prepared for joining. Also, a series of preliminary tests were performed to determine the optimum parameters of welding. The appropriate range for the studied parameters was identified after achieving an acceptable weld penetration without cracks on the sample sheets. During the TIG gas welding process, the joint was protected by argon gas at a rate of 6% and a purity percentage of 99.99%. Welding currents of 75-85 A were used for Inconel 617 during weldingThe laser welding of Inconel 617 superalloy was performed as single pulse welding using an Nd: YAG laser welding device, model UW-300A. In laser welding, the focus position was fully focused, and the laser beam diameter was 0.5 mm with a focal length of 30 mm (constant laser diameter). The maximum power, frequency, pulse width, and welding speed were set at 3600 W, 8 Hz, 5 ms, and 1 mm/s, respectively. To obtain better laser weld quality, the welding parameters are kept constant. To investigate and evaluate the strength of welded sample joints, a GOTECH-GT-7001 tensile tester was used. Samples were cut to the desired dimensions to prepare tensile specimens and then subjected to loading. The tensile test was performed at a rate of 5 mm/min at room temperature. Also, cryogenic tensile tests were performed according to ASTM E8 (2022) standards for the laser-welded samples to evaluate mechanical properties such as tensile properties. Tensile tests were performed using an Instron 5982 tester at room temperature and a cryogenic temperature of -192 °C. The liner extension rate was kept at 1 mm/min. Due to experimental setup limitations, the present study did not perform tensile tests at temperatures below 143 Kelvin. Tensile tests were performed with 10 seconds loading time. A schematic image of performing the cryogenic test (a) and a real image of the laboratory test conditions (b) can be seen in **Figure 1**.

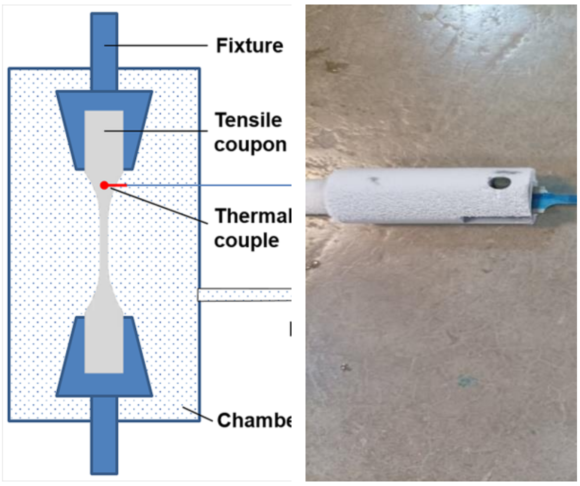

(a) **(b)**

Figure 1. a) Schematic image of the cryogenic test, **b)** Real image of the laboratory test conditions

Results and Discussion

TIG Welding with Argon Gas

Tensile testing provides crucial insights into the strength and ductility of materials under uniaxial tensile stresses. For testing, samples were prepared perpendicular to the weld line so that the weld seam bisected the gauge length. A constant strain rate of 0.001/s was maintained during all tensile tests. Moreover, waterjet or abrasive waterjet cutting methods were utilized to extract test specimens to preclude influences from mechanical machining on the fusion zone that could potentially impact results. A minimum of four replicate tensile specimens were tested for each weld condition to ensure the accuracy of the reported ultimate tensile strength values.

Figure 2 exhibits a 14×2 mm Inconel 617 tensile specimen featuring a double-sided TIG weld fusion zone produced using an argon shielding gas and 316 stainless steel filler wire. This sample typifies those used for quantification of tensile properties.

Figure 2. Inconel 617 using double-sided TIG welding with argon gas and 316 stainless steel filler

Table 2 documents the yield and ultimate tensile strengths for as-received and TIG welded Inconel 617. The base metal possesses considerably higher strengths than the TIG welds. This strength reduction likely stems from deleterious phase precipitates along the bond interfaces, as Liu et al. [27] noted. Additionally, rapid solidification and cooling induce thermal strains in the fusion zone that remain upon cooling to ambient temperatures, degrading strength relative to the pristine base metal, according to Kumar and Pandey [28]. Microstructural evolution from phase transformations within the spatially diverse fusion zone, heat-affected zone, and base metal regions may also contribute to strength losses [29]. Another potential factor is the depletion of beneficial alloying elements, including 21% chromium and 8% molybdenum during TIG welding, which otherwise fortify Inconel 617 through protective chromium oxide scales, and intermetallic precipitates containing chromium, molybdenum, titanium nitride, and titanium carbide as described by Ranjbar et al. [30] As such, the heat of the weld zone and similar cases can reduce the tensile strength in welded samples.

Based on the results in **Table 2**, it can be concluded that double-sided welding using Inconel 617 increases the final strength. It can be said that double-sided welding increases the overlap of the joined pieces, and this overlap on both sides of the joint improves the mechanical properties. In addition, double-sided welding reduces residual stresses resulting from the rolling of the base metal and also causes grain refinement in the base metal in the welded region, which improves the mechanical properties and final strength [31].

According to the results in **Table 2**, using filler material improves the mechanical properties of Inconel 617 alloy. In studies such as Kumar and Balasubramanian [1], ERNiCrCoMo-1 was used as a filler material, which reported lower tensile strength compared to this study. Regarding the increase in tensile strength when using 316 stainless steel filler, it can be said that the higher molybdenum concentration in 316 stainless steel results in a higher density of molybdenum-rich carbide phases (Mo6C). The molybdenum-rich phases increase precipitation strengthening and cause a hardening effect. The higher density of secondary molybdenum-rich phases also provides a hardening effect on the weld zone, which is reflected in the hardness results. The large atomic size of molybdenum compared to other alloying elements also induces significant lattice distortion, leading to increased hardness [21, 32]. Additionally, elements like molybdenum enrich the austenitic matrix with molybdenum-rich carbide phases due to their limited solubility, increasing hardness through precipitation hardening.

Table 2. Yield strength and tensile strength results of Inconel 617 samples in TIG welding

Alloy Type	Dimensions (mm)	Welding Type	Filler	Maximum Load (kN)	Yield Strength (MPa)	Tensile Strength (MPa)
Inconel 617 Raw	14x2	--	--	12.38	478.6	709.25
Inconel 617	14x2	One-sided	No Filler	7.32	312.39	325.68
Inconel 617	14x2	One-sided	Stainless Steel 316	8.52	477.33	445.67
Inconel 617	14x2	Two-sided	Stainless Steel 316	7.40	414	548.67

In **Table 3**, the tensile test results of the welded samples can be observed. As can be seen, failure occurs at the joint in most samples. It can be stated that the residual stress generated in the weld zone is mostly compressive for the samples. Additionally, since the laboratory conditions were not ideal, it facilitated the formation of micro-voids in the weld zone, which reduced the weld strength and caused failure at the joint for most samples. Moreover, the formation of intermetallic compounds in the weld zone introduces brittleness in that region, which can also lead to fracture failure.

Table 3. Tensile test results of welded Inconel 617 samples in argon arc welding.

Alloy Type	Dimensions (mm)	Welding Type	Maximum Load (kN)	Ultimate Strength (MPa)	Fracture Location
Inconel 617	14x2	Argon Two-sided	8.88	636	Connection point
Inconel 617	14x2	Argon Two-sided	8.23	480	Connection point

Laser Pulse Welding

The tensile strength and yield stress results of Inconel 617 samples welded using laser can be seen in **Table 4**. In laser welding, the filler wire is mainly melted by the radiation energy from the weld pool, and the wire adheres to the melt pool due to the high melting point and high viscosity of the nickel filler metal. As shown in **Table 4**, the base metal's tensile strength was higher than the welded state. This can be attributed to the laser energy being transferred to the deeper section of the weld metal, creating a deep keyhole and lack of coalescence between the sidewall and filler metal, resulting in lower tensile strength of the laser welded Inconel compared to the base metal [6]. Laser welding can be improved by being performed at higher weld pool temperatures and for longer durations. Due to the bridging molten metal transfer mode, there can be sufficient time for the groove to fuse and for the filler to transfer, resulting in good coalescence.

Table 4. Yield stress and tensile strength results of Inconel 617 samples in laser welding

Alloy Type	Dimensions (mm)	Welding Type	Filler	Maximum Load (kN)	Yield Strength (MPa)	Tensile Strength (MPa)
Inconel 617 Raw	14x2	--	--	14.49	501.76	748.21
Inconel 617	14x2	One-sided	With Filler	10.69	500.86	534.15
Inconel 617	14x2	Two-sided	With Filler	9.34	487.34	587.43

Subsequently, tensile specimens were prepared according to ASTM-E8 standards using 1.5 mm thick Inconel 617 sheets. **Table 5** shows the cryogenic tensile test results for Inconel 617, where YS is yield strength, UTS is ultimate tensile strength, and EL is elongation.

Table 5. Cryogenic tensile test results for Inconel 617

Dimensions	Welding Type	Ultimate Load (N)	Ultimate Tensile Strength (N/mm²)	Yield Strength (0.2%) (N/mm²)	Elongation (%)	Temperature (°C)
6.08×1.57	One-sided Laser	6229	652	498	8	-192
5.67×1.57	One-sided Argon	8299	932	345	36	-192
5.89×1.57	Two-sided Laser	6169	667	436	8	-192

Based on the results in **Table 5**, at -192 °C, the 1.5 mm thick Inconel sample welded using single-sided argon welding showed higher elongation and ultimate tensile strength. The higher ultimate tensile strength of the single-sided argon-welded Inconel sample can be attributed to its higher dislocation density. Additionally, the higher elongation can be attributed to lower oxide content in this sample.

Conclusion

This study investigated the mechanical properties of similar Inconel 617 welded joints. Argon welding was first performed to join the samples, followed by laser welding for comparison. Based on the results, double-sided argon and laser welding improved the mechanical properties of the sheets compared to single-sided welding. This is because double-sided welding increases the joined pieces' overlap, improving mechanical properties. In most samples, failure occurred in the weld region after loading. This is because residual stresses generated in the welded region were mostly compressive for the samples. Additionally, since laboratory conditions were not ideal, the formation of micro-voids in the weld zone reduced weld strength and caused failure at the joint for most samples. Moreover, the formation of intermetallic compounds introduces brittleness in the weld zone, which can cause fracture failure. Laser welding showed better results than argon welding, which can be attributed to grain growth in the heat-affected zone during argon welding, keeping the coalesced region at high temperatures for a longer time with a slower cooling rate. In laser welding, the coalesced region is smaller due to higher welding speeds and lower heat input.

Acknowledgments: The authors would like to thank Collaborating laboratories for their guidance and support.

Conflict of interest: None

Financial support:. None

Ethics statement: None

References

1. Kumar GP, Balasubramanian KR (2023) Experimental investigation on high-temperature tensile behavior of cold metal transfer pulse multi-control welding of Inconel 617 alloy. Results in Surfaces and Interfaces 10:100100
2. Lee JH, Hwang JH, Park YS, Kim TM, Bae DH, Seo WB, Han JW (2016) Assessing mechanical properties of the dissimilar metal welding between P92 steels and alloy 617 at high temperature. Journal of Mechanical Science and Technology 30:4453-4457
3. Chigilipalli BK, Veeramani A (2022) An experimental investigation and neuro-fuzzy modeling to ascertain metal deposition parameters for the wire arc additive manufacturing of Incoloy 825. CIRP Journal of Manufacturing Science and Technology 38:386-400
4. Zhang Y, Jing H, Xu L, Han Y, Zhao L, Xiao B (2018) Microstructure and mechanical performance of welded joint between a novel heat-resistant steel and Inconel 617 weld metal. Materials Characterization 139:279-292
5. Chigilipalli BK, Veeramani A (2022) Investigations on dry sliding wear behavior of a wire arc additively manufactured nickel-based superalloy. Tribology Transactions 65(5):912-923
6. Sun J, Ren W, Nie P, Huang J, Zhang K, Li Z (2019) Study on the weldability, microstructure, and mechanical properties of thick Inconel 617 plate using narrow gap laser welding method. Materials & Design 175:107823
7. Derakhshi MA, Kangazian J, Shamanian M (2019) Electron beam welding of inconel 617 to AISI 310: Corrosion behavior of weld metal. Vacuum 161:371-374
8. Lim KR, Lee KS, Lee JS, Kim JY, Chang HJ, Na YS (2017) Dual-phase high-entropy alloys for high-temperature structural applications. Journal of Alloys and Compounds 728:1235-1238
9. Salari S, Rahman MS, Polycarpou AA, Beheshti A (2020) Elevated temperature mechanical properties of Inconel 617 surface oxide using nanoindentation. Materials Science and Engineering: A 788:139539
10. Ren W, Lu F, Yang R, Liu X, Li Z (2015) Liquation cracking in fiber laser welded joints of inconel 617. Journal of Materials Processing Technology 226:214-220

11. Srinivas K, Vundavilli PR, Manzoor Hussain M (2022) Experimental investigation on microstructural characterization and mechanical properties of plasma arc welded Inconel 617 plates. High Temperature Materials and Processes 41(1):683-693
12. Tao S, Gao R, Peng H, Guo H, Chen B (2022) High-reliability repair of single-crystal Ni-base superalloy by selective electron beam melting. Materials & Design 224:111421
13. Mandal PK, Saji AM, Lalu AK, Krishnan A, Nair AS, Jacob MM (2022) Microstructural study and mechanical properties of TIG welded Inconel 617 superalloy. Materials Today: Proceedings 62:3561-3568
14. Esmaeili H, Mirsalehi SE, Farzadi A (2018) Vacuum TLP bonding of Inconel 617 superalloy using Ni-Cr-Si-Fe-B filler metal: metallurgical structure and mechanical properties. Vacuum 152:305-311
15. Yin H, Gao Y, Gu Y (2017) Effects of post-welding heat treatment on microstructure and mechanical properties of welding joint of new Ni-Fe based superalloy with Haynes 282 filler metal. Materials Science and Engineering: A 708:118-128
16. Mageshkumar K, Kuppan P, Arivazhagan N (2017) Investigation on microstructure and mechanical properties on pulsed current gas tungsten arc welded super alloy 617. IOP Conference Series: Materials Science and Engineering 6:062032
17. Farahani E, Shamanian M, Ashrafizadeh F (2012) A comparative study on direct and pulsed current gas tungsten arc welding of alloy 617. International Journal on Manufacturing and Material Science 2(1):1
18. Ahmad HW, Hwang JH, Lee JH, Bae DH (2016) An assessment of the mechanical properties and microstructural analysis of dissimilar material welded joint between alloy 617 and 12Cr steel. Metals 6(10):242
19. Kumar A, Pandey C (2023) Structural integrity assessment of Inconel 617/P92 steel dissimilar welds for different groove geometry. Scientific Reports 13(1):8061
20. Cheng H, Kang L, Pang J, Xue B, Du D, Chang B (2021) Effect of the welding position on weld quality when laser welding Inconel 617 Ni-based superalloy. Optics & Laser Technology 139:106962
21. Kumar R, Dey HC, Pradhan AK, Mahapatra MM, Pandey C (2023) Residual stresses study in butt welded joint of Inconel 617 alloy and effect of post weld heat treatment on residual stresses. Proceedings of the Institution of Mechanical Engineers, Part L: Journal of Materials: Design and Applications 237(7):1575-1591
22. Ren W, Swimdeman R (2015) A review paper on aging effects in Alloy 617 for Gen IV Nuclear Reactor applications. J Pressure Vessel Technol 131(2):024002
23. Moslemi N, Redzuan N, Ahmad N, Hor TN (2015) Effect of current on characteristic for 316 stainless steel welded joint including microstructure and mechanical properties. Procedia CIRP 26:560-564
24. Thekkuden DT, Mourad AH, Bouzid AH, Sherif MM (2023) Investigation of expansion percentages and groove inclusions on the performance of welded, expanded, welded-expanded tube-to-tube sheet joints. Journal of Materials Research and Technology 22:2078-2092
25. Jeshvaghani RA, Jaberzadeh M, Zohdi H, Shamanian M (2014) Microstructural study and wear behavior of ductile iron surface alloyed by Inconel 617. Materials & Design (1980-2015) 54:491-497
26. Aqeel M, Gautam JP, Shariff SM (2022) Comparative study on autogenous diode laser, CO2 laser-MIG hybrid and multi-pass TIG welding of 10-mm thick Inconel 617 superalloy. Materials Science and Engineering: A 856:143967
27. Liu W, Lu F, Tang X, Yang R, Cui H (2016) The microstructure evolution and element segregation of Inconel 617 alloy tungsten inert gas welded joint. Journal of Materials Research 31(4):435-442
28. Kumar A, Pandey C (2022) Autogenous laser-welded dissimilar joint of ferritic/martensitic P92 steel and Inconel 617 alloy: Mechanism, microstructure, and mechanical properties. Archives of Civil and Mechanical Engineering 22(1):39
29. Liu W, Lu F, Yang R, Tang X, Cui H (2015) Gleeble simulation of the HAZ in Inconel 617 welding. Journal of Materials Processing Technology 225:221-228
30. Ranjbar K, Dehmolaei R, Amra M, Keivanrad I (2018) Microstructure and properties of a dissimilar weld between alloy 617 and A387 steel using different filler metals. Welding in the World 62:1121-1136
31. Xu H, Liu W, Lu F, Wang P, Ding Y (2017) Evolution of carbides and its characterization in HAZ during NG-TIG welding of Alloy 617B. Materials Characterization 130:270-277
32. Abdel Rahman MS, Abdel Raheem NA, El Koussy MR (2014) Effect of heat input on the microstructure and properties of dissimilar weld joint between Incoloy 28 and superaustenitic stainless steel. Acta Metallurgica Sinica (English Letters) 27:259-266